ORIGINAL RESEARCH

Mesenchymal folliculin is required for alveolar development: implications for cystic lung disease in Birt-Hogg-Dubé syndrome

Ling Chu,[1,2] Yongfeng Luo,[2] Hui Chen,[2] Qing Miao,[2] Larry Wang,[2] Rex Moats,[2] Tiansheng Wang,[1] John C Kennedy,[3] Elizabeth P Henske,[3] Wei Shi [2]

► Additional material is published online only. To view please visit the journal online (http://dx.doi.org/10.1136/thoraxjnl-2019-214112).

[1]The Third Xiangya Hospital, Central South University, Changsha, Hunan, China
[2]The Saban Research Institute, Children's Hospital Los Angeles, Keck School of Medicine, University of Southern California, Los Angeles, California, USA
[3]Division of Pulmonary and Critical Care Medicine, Brigham and Women's Hospital, Harvard Medical School, Boston, Massachusetts, USA

Correspondence to
Dr Wei Shi, The Saban Research Institute, Children's Hospital Los Angeles, Los Angeles, CA 90027, USA;
WShi@chla.usc.edu

EPH and WS are joint senior authors.

Received 23 September 2019
Revised 13 February 2020
Accepted 18 March 2020
Published Online First
1 April 2020

ABSTRACT

Background Pulmonary cysts and spontaneous pneumothorax are presented in most patients with Birt-Hogg-Dubé (BHD) syndrome, which is caused by loss of function mutations in the *folliculin* (*FLCN*) gene. The pathogenic mechanisms underlying the cystic lung disease in BHD are poorly understood.

Methods Mesenchymal *Flcn* was specifically deleted in mice or in cultured lung mesenchymal progenitor cells using a Cre/loxP approach. Dynamic changes in lung structure, cellular and molecular phenotypes and signalling were measured by histology, immunofluorescence staining and immunoblotting.

Results Deletion of *Flcn* in mesoderm-derived mesenchymal cells results in significant reduction of postnatal alveolar growth and subsequent alveolar destruction, leading to cystic lesions. Cell proliferation and alveolar myofibroblast differentiation are inhibited in the *Flcn* knockout lungs, and expression of the extracellular matrix proteins Col3a1 and elastin are downregulated. Signalling pathways including mTORC1, AMP-activated protein kinase, ERK1/2 and Wnt-β-catenin are differentially affected at different developmental stages. All the above changes have statistical significance ($p<0.05$).

Conclusions Mesenchymal Flcn is an essential regulator during alveolar development and maintenance, through multiple cellular and molecular mechanisms. The mesenchymal *Flcn* knockout mouse model provides the first in vivo disease model that may recapitulate the stages of cyst development in human BHD. These findings elucidate the developmental origins and mechanisms of lung disease in BHD.

Key messages

What is the key question?

► The mechanisms underlying pulmonary cystic lesions in Birt-Hogg-Dubé (BHD) syndrome are unclear.

What is the bottom line?

► Mesenchymal folliculin is an essential regulator for alveolar development and/or maintenance through the promotion of alveolar myofibroblast growth and extracellular matrix protein expression. In human BHD, these mechanisms may result in alveolar hypoplasia, subsequent cystic lesions and pneumothorax.

Why read on?

► The fact that mesenchymal inactivation of folliculin during lung development may be responsible for cystic lung disease in BHD syndrome is novel and unexpected, and could lead to new strategies to prevent pneumothorax in patients with BHD syndrome. There may be implications for other diseases associated with pneumothorax.

INTRODUCTION

Germline loss of function mutations in the *Folliculin* (*FLCN*) gene cause Birt-Hogg-Dubé syndrome (BHD), an autosomal dominant syndrome.[1] Patients with BHD syndrome can develop skin fibrofoliculomas, pulmonary cysts and pneumothorax, and renal cell carcinoma and renal cysts.[2] Pulmonary cysts (multiple and bilateral) develop in 80%–100% patients with BHD syndrome, 76% of whom develop a pneumothorax. BHD is one of the most common causes of familial spontaneous pneumothorax.[3 4] The pathogenic mechanisms underlying cystic lung disease in BHD are poorly understood.

Folliculin, the *FLCN*-encoded protein, shares little sequence similarity with any other known proteins.[1] Studies in cultured cells show that FLCN forms a complex with FLCN-interacting proteins 1 and 2 (FNIP1 and FNIP2), and 5′-AMP-activated protein kinase (AMPK), which may regulate several growth factor signal pathways including mTOR and MEK-ERK in a variety of cellular processes.[5–12]

Renal cell carcinoma in BHD follows the Knudson two-hit tumour suppressor gene model, with a germline-inactivating mutation of one allele of *FLCN* and a somatic mutation inactivating the remaining wild-type allele, suggesting that inactivation of both alleles is required for renal cell carcinoma pathogenesis. In mice, conventional homozygous deletion of *Flcn* leads to embryonic lethality, while heterozygous *Flcn* deletion causes kidney tumours in adult mice but no lung pathology.[9 13] It was previously reported that lung epithelial-specific deletion of *Flcn* results in moderate alveolar enlargement in adult, but no pulmonary cysts resembling human BHD.[8]

Using in situ hybridisation[14] or single cell RNA-seq (LungMAP.net), *Flcn* mRNA has been detected in human lung mesenchymal cells from the fetal

► http://dx.doi.org/10.1136/thoraxjnl-2019-213225
► http://dx.doi.org/10.1136/thoraxjnl-2020-214861

To cite: Chu L, Luo Y, Chen H, *et al*. *Thorax* 2020;**75**:486–493.

developmental stages to adulthood. In cultured human fetal lung fibroblasts, inactivation of *Flcn* results in downregulation of Wnt signalling,[15] which is known to be critical for lung development and homeostasis. These findings suggest that mesenchymal Flcn could be important for lung development. However, the roles of mesenchymal Flcn in lung alveolar development and maintenance have never been investigated in vivo. We deleted *Flcn* in mesoderm-derived mesenchymal cells using the *Dermo1-Cre* driver. The *Flcn* conditional knockout (KO) mice develop lesions in multiple organs and die in the first month after birth. Here, we focus on the dynamic changes of lung development and maintenance in these mice, including cellular and molecular abnormalities, and changes in cell proliferation, differentiation and extracellular matrix (ECM) composition. Taken together, these findings reveal a critical role for mesenchymal folliculin in lung development, with key implications for the pathogenesis of cystic lung disease in patients with BHD syndrome.

MATERIAL AND METHODS

Mice

Dermo1-Cre and Floxed-*Flcn* (*Flcn*$^{f/f}$) mice were provided by Dr David Ornitz at Washington University-St. Louis and Dr Laura Schmidt at the National Cancer Institute, respectively.[11 16] Mice were bred in the C57BL/6J stain background and housed in pathogen-free conditions at the animal facility of Children's Hospital Los Angeles. Timed mating between *Flcn*$^{f/+}$ and *Dermo1-Cre*/*Flcn*$^{f/+}$ mice generated mesenchymal *Flcn* homozygous KO mice (*Dermo1-Cre*/*Flcn*$^{f/f}$), *Flcn* heterozygous KO mice (*Dermo1-Cre*/*Flcn*$^{f/+}$), wild type mice (*Flcn*$^{+/+}$) and other control mice (*Flcn*$^{f/f}$ or *Flcn*$^{f/+}$). Because lung structure in other control mice is normal same as wild type mice (*Flcn*$^{+/+}$), they are all included in wild type group in this study. Mouse genotypes were determined by PCR using the primers: 5′-GTTGTCTGGAGT GCTACTTAGTCAGG-3′, 5′-CAACACCCCAGCATCCAG-3′ and 5′CAGCTCCCTCTACCCAGACA-3′ for *Flcn*, 5′-GCAA CATTTGGGCCAGCTAAAC-3′ and 5′-CCGGCATCAACG TTTTCTTTTC-3′ for *Dermo1-Cre*. Mouse X-ray images were taken at the small animal imaging core at Children's Hospital Los Angeles. Mouse studies followed the National Institute of Health Animal Research Advisory Committee Guideline.

Histology and morphometric analysis

Mice at different ages were weighed and euthanised. Tissue samples were then isolated for either fixation in 4% buffered paraformaldehyde or storage at −80°C by snap freezing. For morphology, lung tissues were inflated under 25 cm H_2O pressure through intratracheal cannulation prior to fixation. The fixed tissues were embedded in paraffin and sectioned with 5 µm thickness. These tissue sections were used for H&E staining or immunohistochemistry. For lung morphometric analysis, five sections of each tissue were randomly chosen at approximately 200 µm intervals, and more than 128 measurements were performed per sample. At least five lungs from both males and females per genotype were analysed at each time point. The mean linear intercept (MLI) was used to measure average size of alveoli.[17] Results were analysed with independent sample t-test to compare the differences between mean values and considered significant if $p<0.05$.

Immunofluorescence staining, detection and image analysis

Tissue section was deparaffinised and rehydrated, and antigen retrieval was performed by boiling the tissue slides in Tris-EDTA buffer (pH 9.0) for 25 min. After blocking with 10% donkey serum for 1 hour, the tissue sections were incubated with the following primary antibodies overnight at 4°C: goat anti-Pecam1 and Scgb1a1 (sc-1506 and sc-9772, Santa Cruz), Col3a1 (NBP1-26547, Novus) and GFP (G095, Abm); rabbit anti-Sftpc (WRAB-9337, Seven Hill Bioregeants), Tubb4a (MU178-UC; BioGenex), Plin2 (LS-B3121, LSBio), elastin (provided by Dr Robert Mecham at Washington University),[18] Pdpn (DSHB at the University of Iowa), Acta2 (A2547; Sigma Aldrich) and active caspase 3 (#9661, CST). Donkey secondary antibodies conjugated with Alexa Fluro 488, Alexa Fluro 594 or Alexa Fluro 647 (ThermoFisher) were used, and cell nuclei were counterstained by DAPI in the mounting medium (Vector Laboratories). Fluorescence images were taken using the Zeiss LSM710 confocal microscope at the Imaging Core Facility of Children's Hospital Los Angeles. Immunofluorescence staining was further quantified using NIH ImageJ following published methods[19 20] and was analysed in a blinded fashion. In brief, protein expression of interest was determined by the integrated density (sum of grey values of all selected objects) and normalised to the area stained by DAPI in the same field. A relative ratio of normalised *Flcn* KO integrated density to normalised wild type integrated density was then calculated and presented as mean±SD. Alveolar regions were selected for the immunostaining analysis of Acta2, Sftpc, Pdpn, Pecam1 and Plin2, while bronchi/bronchioles were used to quantify the immunostaining of Scgb1a1 and Tubb4a.

Western blot

Detection of proteins in tissue lysates by western blot has been previously described.[21] Briefly, equal amounts (40 µg) of total tissue lysates were separated in precast PAGE gels (4%–15% gradient; Bio-Rad, Hercules, California) and transferred into polyvinylidene difluoride membrane using Bio-Rad's Trans-Blot Turbo System. Proteins of interest were detected using the following specific antibodies from Cell Signaling Technology: rabbit antiphospho-S6 (Ser235/236) and mouse anti-S6 (4858 and 2317), rabbit antiphospho-ERK1/2 and ERK1/2 (9101 and 4695), rabbit antiphospho-AMPKα and mouse anti-AMPKα (50 081 and 2793), rabbit anti-active β-catenin and total β-catenin (1980 and 8480), and mouse anti-Actb1 (3700). Rabbit anti-FLCN antibody was provided by Dr Arnim Pause at McGill University.[22] Antibodies for Col3a1, Elastin and Acta2 were the same ones used for immunostaining. At least three independent mouse lung samples per genotype were analysed. The densitometric intensities of the detected protein bands were quantified using ImageJ and normalised by protein loading controls.

Mouse lung cell proliferation

To detect cell proliferation in vivo, ethynyl-deoxyuridine (EdU) was used to label proliferating cell nuclei with DNA synthetic activities.[23] Briefly, mice were intraperitoneally injected with EdU (5 mg/kg body weight) 3 hours before tissue harvest and detected with Alexa Fluor azide (ThermoFisher). Cell nuclei were counterstained with DAPI. The images (four random fields per slide from a total of four slides per mouse) were analysed using ImageJ to measure the ratio of EdU-labelled nuclei to total DAPI-stained nuclei as an index of cell proliferation. Experiments were repeated more than three mice per genotype.

Lung mesenchymal progenitor cell isolation, Flcn deletion and proliferation

Lung mesenchymal progenitor cells with genotype of *Flcn*$^{f/f}$ were isolated and cultured using a modified method.[24] Briefly,

a deblooded *Flcn*$^{f/f}$ lung lobe was minced and digested with dispase/collgenase for 40 min at 37°C. The digested cells were filtrated through a 70 µm strainer, pelleted and resuspended in culture medium (αMEM, 20% fetal bovine serum(FBS), 2 mM glutamine and 55 µM 2-mercaptoethanol). The cells were then plated at low density (~10^4/100 mm dish). After 2 weeks, colonies of lung mesenchymal stem cells were formed, passaged and validated by their negative staining for Cdh1 and Pecam1 (data not included). The cells (<10 passages) with 80%–90% of confluence were infected with Cre expressing adenovirus (Ad-Cre) or control virus (Ad-GFP) in the absence of serum for 6 hours.[25] The cells were then cultured in medium containing 20% FBS and 10 µM EdU for 6 hours and measured for proliferation as described above.

Statistical analysis

All experiments were repeated at least three times. The quantitative data were presented as mean±SD. Most statistical analyses were performed using analysis of variance or two-tail independent sample t-test with assumption of equal variances. The nonparametric logrank (Mantel-Cox) test was used for comparing mouse survival curves. Actual p values are presented except that p values are less than 0.001 ($p<0.001$). $p<0.05$ was considered significant.

RESULTS

Abrogation of Flcn specifically in mesoderm-derived mesenchymal cells results in retardation of neonatal growth and later postnatal lethality

To determine the functions of mesenchymal Flcn in organ development and maintenance, we specifically knocked out *Flcn* gene in mesoderm-derived mesenchymal cells of multiple organs using *Dermo1-Cre* driven DNA recombination of floxed-*Flcn* (*Flcn*$^{f/f}$) in mice. The newborn mice had the expected litter size and the ratios of genotypes and genders. The pups of homozygous *Flcn* conditional KO with genotypes of *Dermo1-Cre/Flcn*$^{f/f}$) had smaller body size than their wild type littermates even at postnatal day 1 (figure 1A). This difference in body size became more obvious at later time points (figure 1B), confirming that *Flcn* KO mice have significant growth retardation. Abnormalities in skeletal bone structures, examined by frontal and lateral X-ray (figure 1C), were not detected. This growth abnormality was not seen in mice with heterozygous *Flcn* deletion (*Dermo1-Cre/Flcn*$^{f/+}$) up to 6 months age (data not shown). Most homozygous *Flcn* KO mice died suddenly around postnatal week 2, although some survived to more than 1 month of age (figure 1D). No sex difference in survival was detected. The cause for the early lethality is not clear. At autopsy, significant lesions in major organs were not evident except a pale appearance of the lung. Histologically, pulmonary oedema and focal cardiomyocyte degeneration were seen (online supplementary figure 1).

Mesenchymal Flcn is essential for lung alveolar growth and maintenance

It is not known whether the pulmonary cysts in patients with BHD syndrome are the result of postdevelopmental destruction of alveoli or of alveolar developmental defects, or both. BHD-associated pulmonary cysts have been reported at gestational age 34 weeks,[26] suggesting a developmental origin. To address this in the *Flcn* KO model, lung morphology was analysed at multiple time points. The saccular structure of prenatal E18.5 lung in the *Flcn* KO mice was comparable with that of wild type littermates (figure 2), suggesting that fetal airway branching morphogenesis is not affected by loss of Flcn. In contrast, postnatal alveolar formation was significantly reduced in the *Flcn* homozygous KO mice, detected at early alveolarisation stage (P7,

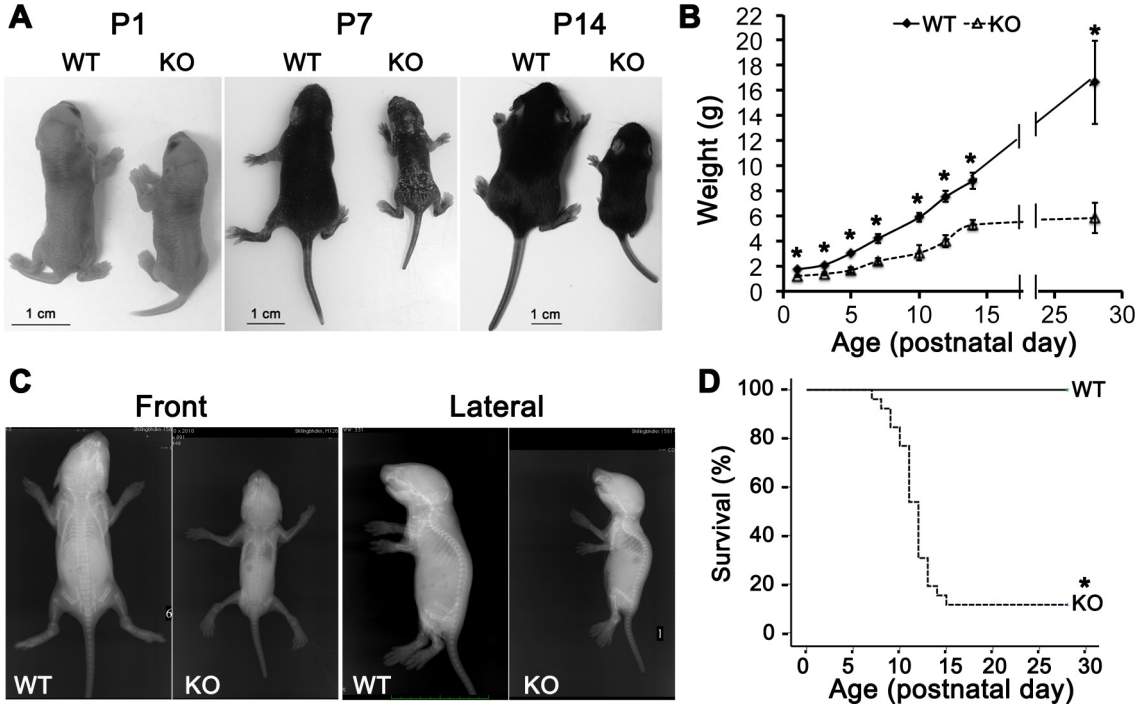

Figure 1 Deletion of *Flcn* in mesoderm-derived cells resulted in retarded body growth and early lethality. (A) Comparison of the body sizes between the Flcn conditional knockout (KO) mice and their littermate wild-type (WT) controls at different postnatal ages. (B) Growth curves of *Flcn* KO mice and their WT littermates (n=20 for ages of <P12, n=10 for P14 and n=5 for P28). *p<0.001. (C) Front and lateral X-ray images of the mice at P7. (D) Altered survival for the *Flcn* KO mice shown by their Kaplan-Meier curves (n=30 per group, *p<0.001 logrank test). P12, postnatal day 12.

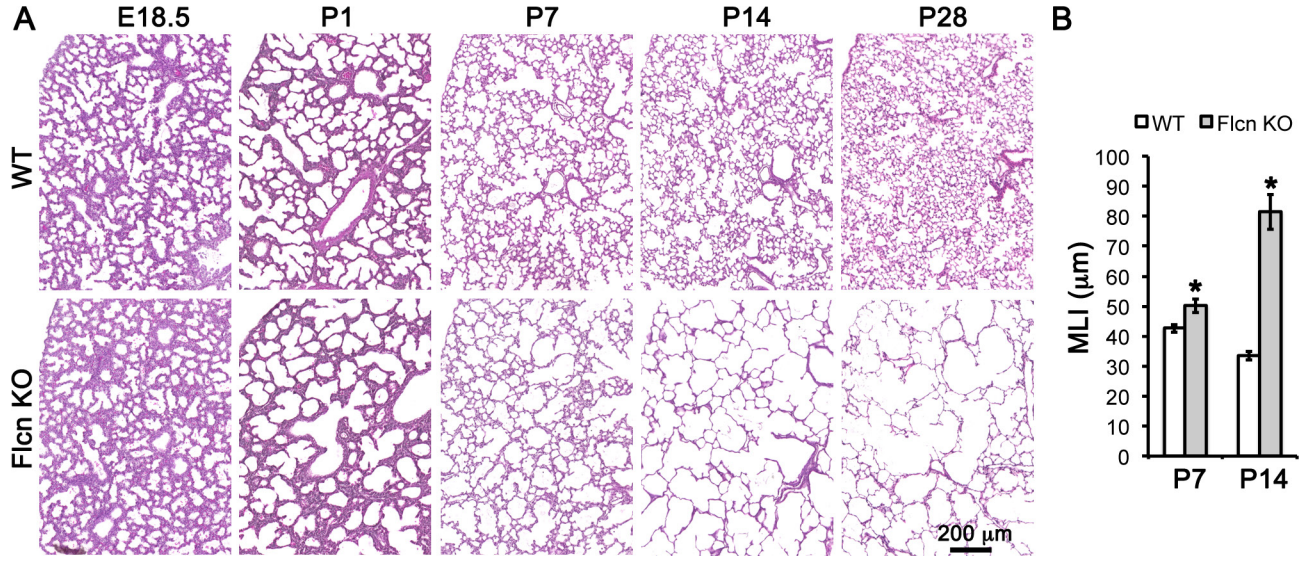

Figure 2 Dynamic changes of alveolar structures in the *Flcn* KO mouse lungs. (A) H&E stained lung sections; (B) Quantification of alveolar sizes by measuring mean linear intercept (MLI; n≥5 per group, *p<0.05 (0.007 and 0.001, respectively). KO, knockout; WT, wild type.

figure 2), which was also quantitatively validated by measuring MLI (42.7±1.3 μm in wild type vs 50.1±2.2 μm in *Flcn* KO, figure 2). Moreover, at the late stage of alveolar development (P14–P28), further enlargement of alveoli (MLI: 33.4±1.4 μm in wild type vs 81.4±5.8 μm in *Flcn* KO, figure 2) was observed. In particular, focal cystic lesions with destructed alveolar walls were prominent in the *Flcn homozygous* KO mouse lungs at P28 (figure 2). Interestingly, heterozygous deletion of *Flcn* did not cause significant alteration of lung structure at 4 months of age (online supplementary figure 2).

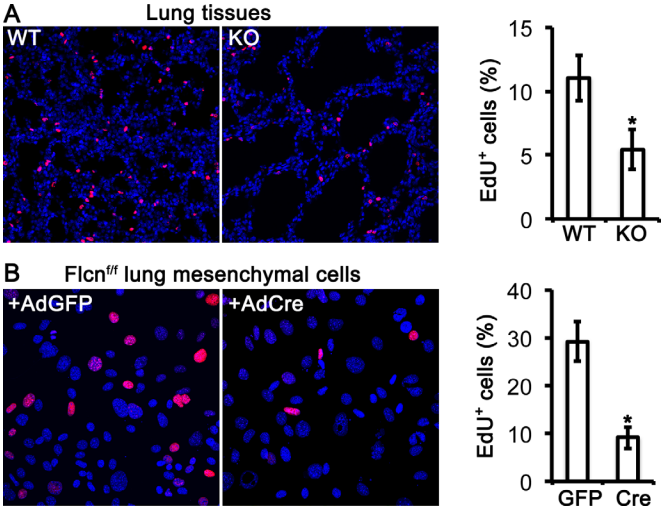

Figure 3 Abrogation of Flcn resulted in reduced lung cell proliferation. (A) Cell proliferations in P10 mouse lungs were detected using EdU incorporation (red) to label proliferating cell nuclei with DNA synthetic activities as shown by confocal images (left); all nuclei were counterstained with DAPI (blue). The percentage of EdU-positive cells was quantified (right). *p=0.001. (B) Proliferations of cultured lung mesenchymal cells with versus without *Flcn* deletion were also measured by EdU labelling, shown as confocal images (left) and percentage of EdU-positive cells (right). *p<0.001. EdU, ethynyl-deoxyuridine; KO, knockout; WT, wild type.

Loss of mesenchymal Flcn leads to decreased cell proliferation and myofibroblast differentiation during alveolarisation

To further understand the cellular mechanisms underlying the above lung phenotypes, cell proliferation, differentiation and apoptosis were compared between *Flcn* KO and wild type littermate controls at the early alveolarisation stage (P10). Using an EdU labelling approach, a significant reduction of cell proliferation in the *Flcn* KO mouse lung was detected (5.4%±1.5% in *Flcn* KOs vs 11.0%±1.7% in wild type littermates, figure 3A). The direct impact of Flcn on mesenchymal cell proliferation was further examined in vitro. Primary lung mesenchymal cells from floxed-*Flcn* mice were isolated and cultured. The cells were then infected with adenoviruses expressing either Cre or green fluorescent protein (GFP) control. The cells with Cre-mediated *Flcn* deletion in vitro had a significant reduction of cell proliferation in comparison with cells infected with adenoviral control (GFP expression, figure 3B), which was comparable with cells without adenoviral infection. Apoptotic cells in the lung, detected by immunostaining for activated-caspase3, were rare in both *Flcn* KO and wild type mice (online supplementary figure 3), suggesting that reduced cell proliferation rather than increased cell death may contribute to decreased alveolar growth.

Alveolar myofibroblast differentiation and migration are the driving forces for new alveolar septa formation and subsequent expansion of the alveolar surface, which spikes during early postnatal alveolarisation in mice. Therefore, we next examined alveolar myofibroblasts by immunostaining P10 lungs with Acta2 (α-smooth muscle actin). In the lungs with *Flcn* KO as validated by both immunofluorescence staining and western blot (figure 4A and C), alveolar myofibroblasts were strikingly reduced while the number of lipofibroblasts (Plin2, figure 4A–B) was not affected, suggesting that Flcn is specifically involved in alveolar myofibroblast differentiation. To validate this change, primary lung mesenchymal progenitor cells with a *Flcn*$^{f/f}$ genotype were infected with adenoviral Cre or GFP, followed by treatment with TGFβ1 (5 ng/mL), which is known to promote myofibroblast differentiation. Twenty-four hours later, the cells with AdCre-mediated *Flcn* deletion had reduced TGFβ1-induced *Acta2* expression at the mRNA level compared with AdGFP control

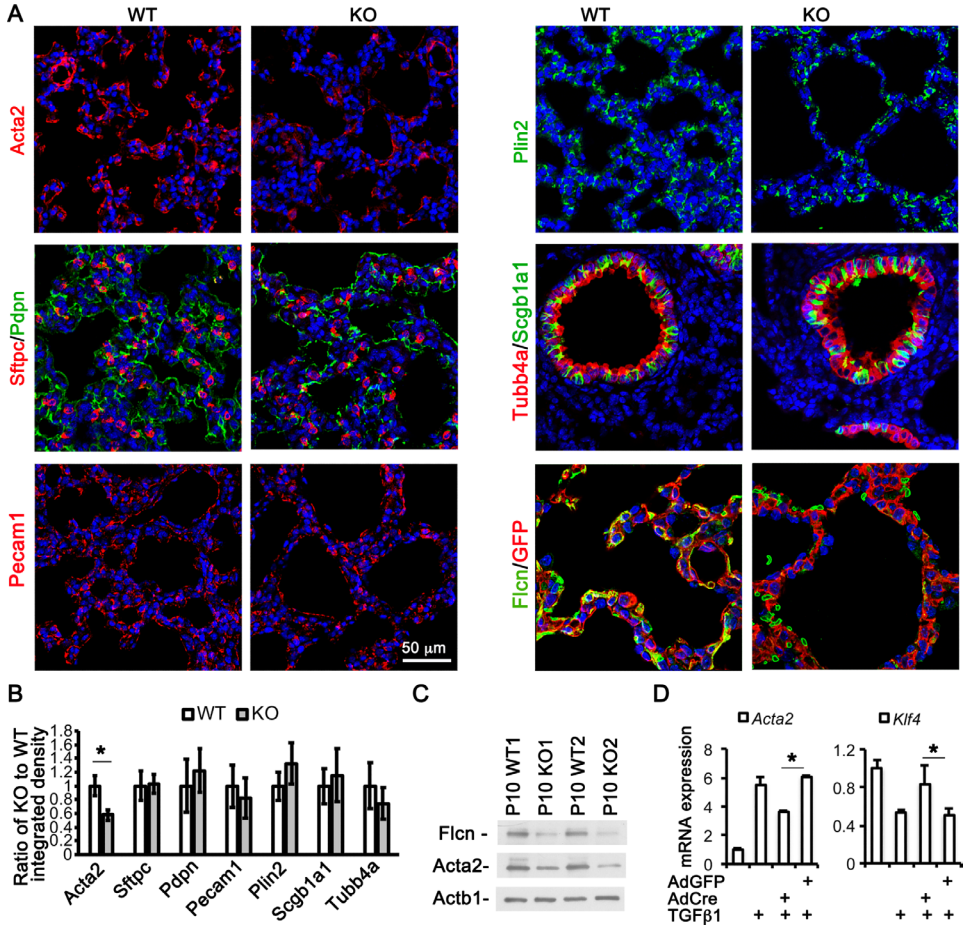

Figure 4 Deletion of mesenchymal Flcn altered alveolar myofibroblast differentiation. (A) Comparison of alveolar cell types between P10 *Flcn* knockout (KO) mouse lungs and the wild type (WT) littermate controls. The used cell markers were Acta2 for myofibroblasts, Sftpc and Pdpn for type 2 and type 1 alveolar epithelial cells, respectively, Pecam1 for endothelial cells, Plin2 for lipofibroblasts, Tubb4a and Scgb1a1 for airway ciliated cells and Club cells, respectively. Loss of Flcn expression (green) in lung mesenchymal cells marked by GFP-stained cells (red) from the *Dermo1-Cre/mT-mG/Flcn*$^{f/f}$ mouse lungs was detected. (B) The integrated intensity of the above immunostaining from at least six different fields per sample and three samples per genotype was measured and normalised by the DAPI staining area. Difference between WT and *Flcn* KO samples was analysed and presented as the ratio (mean±SD), *p=0.006. (C) Western blot analysis was used to validate reductions of Acta2 and Flcn in P10 *Flcn* KO lung tissue lysates. Actb1 was a loading control. (D) Real-time PCR to detect gene expression at the mRNA level for Acta2 and Klf4 in cultured *Flcn*$^{f/f}$ lung mesenchymal cells, which were infected with indicated adenoviral vectors and subsequently treated with TGF-β1 (5 ng/mL) for 24 hours. *p<0.05 (0.001 and 0.044, respectively).

(figure 4D). More interestingly, inhibition of *Klf4* mRNA expression by TGFβ1 did not occur in the cells when *Flcn* was deleted (figure 4D), suggesting that Flcn may be involved in regulating *Klf4* (a key transcription repressor for myogenic protein expression) and subsequent myofibroblast differentiation. However, type II and type I alveolar epithelial cells in P10 lungs, detected by their cellular markers (Sftpc and Pdpn, respectively), were not changed (figure 4A–B). The number and distribution of two major proximal airway epithelial cells, ciliated cells and Club cells (Tubb4a and Scgb1a1, respectively in figure 4A–B), were also comparable between *Flcn* KO and wild type control mice at P10. Furthermore, the alveolar capillary network, detected by Pecam1-endothelial staining, was relatively normal in *Flcn* KO lung alveolar septa (figure 4A–B), further highlighting the specificity of the changes in myofibroblasts.

Abrogation of mesenchymal Flcn inhibits production of major ECM proteins in alveolar walls

Both cells (including epithelial and interstitial cells) and extracellular matrices are important components of alveolar septa. Since alveolar septal formation was reduced in the *Flcn* KO lung, we examined ECM proteins, focusing on collagen and elastin. Collagen I and III are the major fibre collagens in the lung. By real-time PCR, we found that expression of *Col3a1*, but not *Col1a1*, at the mRNA level was significantly reduced in the *Flcn* KO lung only during alveolar growth (P10, figure 5A). Similarly, *elastin* (*Eln*) expression at the mRNA level decreased significantly during alveolarisation (P10), but not at the end of alveolar growth (P28, figure 5A). Reductions of Col3a1 and elastin in *Flcn* KO lungs were further confirmed at the protein level by immunoblotting and immunofluorescence staining (figure 5B–D). Interestingly, elastin protein in lung tissue lysate was reduced at all time points including P28 (figure 5B–C), suggesting that a defect of deposited elastin protein from early alveolar development may persist at later stages even though mRNA expression at later time points does not differ significantly. Immunofluorescence staining also showed thinner and weakly stained collagen III fibres and elastin fibres in alveolar septa (figure 5D). Significant changes in intensity and distribution of other ECM proteins including components of basement membrane such as laminin were not detected (data not shown).

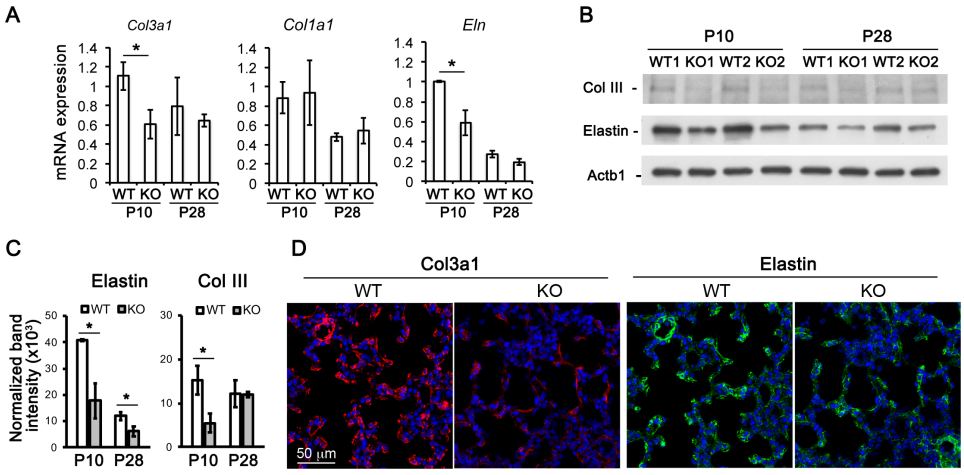

Figure 5 Altered expression of extracellular matrix proteins in the *Flcn* KO lungs. (A) Real-time PCR to detect altered gene expression for *Col3a1*, *Col1a1* and *Eln* at P10 versus p28. *p<0.05 (0.022 for P10 *Col3a1* and 0.039 for P10 *Eln*). (B) Immunoblot to detect changes of collagen III and elastin proteins. (C) Densitometric analysis of the protein bands detected by the immunoblot. Loading control Actb1 was used for normalisation. *p<0.05 (0.020 and 0.040 for P10 and P28 elastin, and 0.036 for P10 Col III). (D) Immunofluorescence staining of P10 Flcn KO lungs and WT controls for Col3a1 and elastin. KO, knockout; WT, wild type.

Mesenchymal Flcn defect results in dynamic changes of cellular signalling

To elucidate the molecular mechanisms underlying the above cellular phenotypes, changes in several signalling pathways were investigated. Previous in vitro studies suggest that Flcn may serve as either positive or negative regulator for mTORC1,[7 27] in an organ and/or cell type dependent context. By measuring phosphorylation of mTORC1 downstream target S6 ribosome protein (pS6), alterations of mTORC1 activity in lung tissue lysate was evaluated. Interestingly, increased S6 phosphorylation (Ser235/236) was detected in P10 *Flcn* KO lung, while decreased S6 phosphorylation was seen in the P28 *Flcn* KO lung (figure 6 and online supplementary table 1). Similar dynamic changes were also seen for phospho-AMPKα and phospho-ERK1/2, suggesting that these pathways may be upregulated by loss of Flcn during alveolar growth directly and/or indirectly but downregulated when alveolar destruction occurs in *Flcn* KO lung.

In addition, downregulation of canonical Wnt signalling, detected by levels of active β-catenin, was consistently detected in *Flcn* KO lungs at multiple stages (figure 6 and online supplementary table 1), consistent with recent evidence from cellular models of Flcn deficiency.[15] The total β-catenin at P28 was also reduced in the *Flcn* KO lung tissue lysates, suggesting that reduced Wnt signalling may contribute to abnormal alveolar growth and/or alveolar maintenance.

DISCUSSION

BHD syndrome is a monogenetic disease caused by germline loss of function mutations in the *FLCN* gene.[2] The clinical manifestations of BHD vary depending on the organ(s) involved.[28] In this study, we report that abrogation of mouse *Flcn* in mesoderm-derived mesenchymal cells results in abnormal lung alveolar growth and subsequent pulmonary cystic lesions, one of the common clinical findings in patients with BHD syndrome. Interestingly, a significant reduction of body size and weight in the *Flcn* KO mice was detected; while it has not been reported that human BHD patients have retarded body growth, this may reflect the central role of Flcn in metabolic regulation of multiple tissues including kidney, adipose and bone.[5 29 30] This reveals a novel function of Flcn in body growth during postnatal development.

By analysing the dynamic changes of lung pathology in the *Flcn* KO mice, reduced postnatal lung alveolar growth was found to be the initial defect. Prenatal lung branching morphogenesis was not affected by mesenchymal *Flcn* deletion. A deficiency in alveolar myofibroblast differentiation appears to

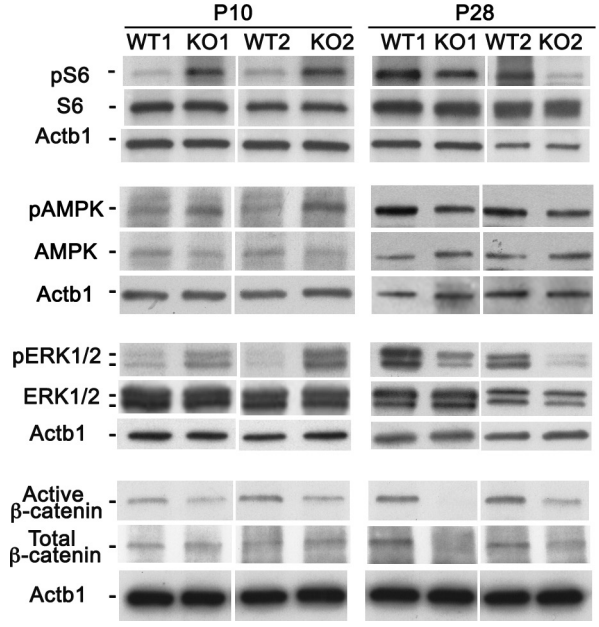

Figure 6 Dynamic alterations of some cellular signalling activities in *Flcn* KO lungs, including mTORC1 (pS6), AMPK, MAPK (ERK1/2) and canonical Wnt pathways. pS6, pAMPK and pERK1/2 were increased in *Flcn* knockout (KO) lung tissue lysates compared with the wild type (WT) littermate controls at P10. However, these pathways were decreased in the *Flcn* KO lung at the end of alveolarisation (P28). Active β-catenin was reduced in the *Flcn* KO lungs consistently at both P10 and P28. At least three pairs of samples were analysed, and the ratios of normalised KO to WT band intensities were presented in online supplementary table 1. AMPK, AMP-activated protein kinase.

be a major cellular mechanism underlying the lung abnormalities in this model, as shown by significant reductions of cell proliferation and alveolar myofibroblast differentiation during development. The direct impact of Flcn loss on these cellular changes was further supported by studies using cultured lung mesenchymal progenitor cells. Deletion of *Flcn* in cultured lung mesenchymal cells inhibited transforming growth factor-β1 (TGF-β1)-stimulated α-smooth muscle actin expression. This was accompanied by increased *Klf4* expression, a transcriptional repressor for myogenic gene transcription. Defects in TGF-β-mediated transcription were previously reported in *Flcn*-null mouse embryonic stem cells.[31] Interestingly, Hoshika *et al*[32] reported that primary lung fibroblasts isolated from patients with BHD syndrome also have reduced expression of TGF-β1 and other ECM proteins due to haploinsufficiency of Flcn. Although we did not detect altered TGF-β1 ligand expression in *Flcn* KO lung tissue lysate (online supplementary figure 4), altered intracellular TGF-β signalling may occur in the myofibroblast precursors; further studies would be required to address this.

Wnt/β-catenin signalling represents a second key pathway that is Flcn-regulated in myofibroblasts.[33] Consistently with our recently published discovery that abrogation of Flcn in cultured mouse embryonic fibroblasts and lung fibroblasts inhibits canonical Wnt pathway activity,[15] reduced β-catenin activation was detected in the *Flcn* KO lung tissue both during and after alveolarisation; reduced total β-catenin was only detected at the end of alveolarisation. This is of particular interest since FLCN is known to be required for the exit from cell pluripotency.[34]

In addition to these cellular changes, reduced expression of ECM proteins such as *Col3a1* and *Eln* (key structural components of alveolar septa) could contribute to the alveolar defects in the *Flcn* KO lung. Elastin fibres and collagen fibres are interwoven with glycosaminoglycan and proteoglycans in the alveolar interstitial matrix, in which Col3a1 and Eln are the essential components. Elastin fibres, which have very slow turnover and may last for almost the entire life of a mammal, provide elastic recoil of the lung during respiration. We found a reduction of *Eln* expression at the mRNA level only during alveolar growth. In contrast, elastin protein was continuously reduced even at the end of alveolarisation. This suggests that the lungs of the *Flcn* KO mice may have reduced lung recoil capability and enhanced susceptibility to mechanic stress during later life, further triggering alveolar destruction, consistent with the previously proposed 'stretch hypothesis' for cystic lung disease in BHD.[7 35] Interestingly, germline mutations of COL3A1 result in Ehlers-Danlos syndrome type IV, in which pulmonary cysts and pneumothorax can occur,[36] and mutations in the *ELN* gene have been identified as a cause of emphysema (alveolar destruction and enlargement).[37] In addition, targeted deletion of *FLCN* in human lung fibroblast cells (MRC-5) results in decreased expression of both COL3A1 and ELN as described in our previous publication,[15] demonstrating in vitro that defective COL3A1 and ELN may play important roles in the pathogenesis of lung cysts in BHD. Multiple mechanisms may account for the altered ECM gene expression in BHD, including deficiency of alveolar myofibroblasts during alveolar growth and/or involvement of Flcn in regulating pathways for the gene transcription in fibroblasts, which will need further investigation.

We found that Flcn-regulated metabolic pathways showed distinct alterations at different developmental stages. For example, Flcn is known as a repressor of the master energy sensor AMPK via FNIP.[27 29 38 39] Deletion of Flcn is expected to upregulate AMPK activity. In our *Flcn* KO lungs, AMPK activation, as measured by its phosphorylation, was increased during alveolar formation (P10) and decreased at the end of alveogenesis (P28) when alveolar destruction occurred. Similarly, mTORC1 activity, as measured by phosphorylation of downstream target S6, was increased at P10 and decreased at P28. To our knowledge, this is the first evidence that FLCN's regulation of cellular metabolism is developmentally regulated.

The relationship between cell metabolism and alveolar growth remains unknown. Interestingly, increased mesenchymal mTORC1 during alveolarisation (by deleting its inhibitor Tsc2) can reduce alveolar myofibroblasts and alveolar growth.[40] Previous studies suggest that the relationship between Flcn inactivation and mTORC1 activity is strongly context dependent.[7–10 27 41] For example, pS6 immunostaining is variable depending on cyst size and number in a *Flcn* KO kidney model, with elevated pS6 in large multicyst structure and weak to no pS6 staining in small single cysts.[6] Therefore, the dynamic changes of mTORC1 and AMPK activation in our *Flcn* KO lungs may result from a differential composition of cell types and architectural features.

The roles of MAPK/ERK1/2 in lung alveolarisation and myofibroblast differentiation are also not fully understood. MAPK/ERK1/2 has been shown to associate with hyperoxia-induced alveolar hypoplasia, possibly through abnormal lung fibroblast proliferation.[42] It was also reported that in lung fibroblasts, ERK1/2 activation mediates fibroblast growth factor (FGF) signalling in inhibiting myofibroblast differentiation.[43 44] Whether ERK1/2-mediated signalling enhances fibroblast proliferation and therefore reduced myofibroblast differentiation during alveolarisation needs further investigation.

In summary, we report for the first time that mesenchymal Flcn is an essential regulator during lung development and/or maintenance. This appears to occur through multiple cellular and molecular mechanisms, with differential effects on cellular metabolism at different developmental stages, highlighting the central role of Flcn in lung development. Importantly, in this model, dynamic changes from early defective alveolar growth to subsequent alveolar destruction and cyst-like lesions are observed, providing the first in vivo model that may recapitulate the stages of cyst development in human BHD. These findings elucidate the fundamental pathogenic mechanisms of lung disease in BHD and may also have relevance to other types of cystic lung disease.

Contributors Concept and design, LC, EPH and WS; acquisition of data: LC, YL, HC, QM, TW, RM and WS; analysis and interpretation: LC, JCK, LW, EPH and WS; drafting of the manuscript: LC, JCK, EPH and WS.

Funding The work is funded by National Institute of Health/National Heart, Lung, and Blood Institute grant R01 HL141352-01 (WS).

Competing interests None declared.

Patient consent for publication Not required.

Provenance and peer review Not commissioned; externally peer reviewed.

Data availability statement All data relevant to the study are included in the article or uploaded as supplementary information.

ORCID iD
Wei Shi http://orcid.org/0000-0001-6499-2473

REFERENCES

1 Nickerson ML, Warren MB, Toro JR, *et al*. Mutations in a novel gene lead to kidney tumors, lung wall defects, and benign tumors of the hair follicle in patients with the Birt-Hogg-Dubé syndrome. *Cancer Cell* 2002;2:157–64.
2 Birt AR, Hogg GR, Dubé WJ. Hereditary multiple fibrofolliculomas with trichodiscomas and acrochordons. *Arch Dermatol* 1977;113:1674–7.
3 Liu Y, Xing H, Huang Y, *et al*. Familial spontaneous pneumothorax: importance of screening for Birt-Hogg-Dubé syndrome. *Eur J Cardiothorac Surg* 2019.

4 Gupta N, Kopras EJ, Henske EP, *et al*. Spontaneous pneumothoraces in patients with Birt-Hogg-Dubé syndrome. *Ann Am Thorac Soc* 2017;14:706–13.
5 Chen J, Futami K, Petillo D, *et al*. Deficiency of FLCN in mouse kidney led to development of polycystic kidneys and renal neoplasia. *PLoS One* 2008;3:e3581.
6 Hudon V, Sabourin S, Dydensborg AB, *et al*. Renal tumour suppressor function of the Birt-Hogg-Dubé syndrome gene product folliculin. *J Med Genet* 2010;47:182–9.
7 Khabibullin D, Medvetz DA, Pinilla M, *et al*. Folliculin regulates cell-cell adhesion, AMPK, and mTORC1 in a cell-type-specific manner in lung-derived cells. *Physiol Rep* 2014;2. doi:10.14814/phy2.12107. [Epub ahead of print: 12 Aug 2014].
8 Goncharova EA, Goncharov DA, James ML, *et al*. Folliculin controls lung alveolar enlargement and epithelial cell survival through E-cadherin, LKB1, and AMPK. *Cell Rep* 2014;7:412–23.
9 Hartman TR, Nicolas E, Klein-Szanto A, *et al*. The role of the Birt-Hogg-Dubé protein in mTOR activation and renal tumorigenesis. *Oncogene* 2009;28:1594–604.
10 Petit CS, Roczniak-Ferguson A, Ferguson SM. Recruitment of folliculin to lysosomes supports the amino acid-dependent activation of RAG GTPases. *J Cell Biol* 2013;202:1107–22.
11 Baba M, Furihata M, Hong S-B, *et al*. Kidney-targeted Birt-Hogg-Dube gene inactivation in a mouse model: ERK1/2 and Akt-mTOR activation, cell hyperproliferation, and polycystic kidneys. *J Natl Cancer Inst* 2008;100:140–54.
12 Dunlop EA, Seifan S, Claessens T, *et al*. Flcn, a novel autophagy component, interacts with GABARAP and is regulated by ULK1 phosphorylation. *Autophagy* 2014;10:1749–60.
13 Hasumi Y, Baba M, Ajima R, *et al*. Homozygous loss of BHD causes early embryonic lethality and kidney tumor development with activation of mTORC1 and mTORC2. *Proc Natl Acad Sci U S A* 2009;106:18722–7.
14 Warren MB, Torres-Cabala CA, Turner ML, *et al*. Expression of Birt-Hogg-Dubé gene mRNA in normal and neoplastic human tissues. *Mod Pathol* 2004;17:998–1011.
15 Kennedy JC, Khabibullin D, Hougard T, *et al*. Loss of FLCN inhibits canonical Wnt signaling via TFE3. *Hum Mol Genet* 2019;28:3270–81.
16 Yu K, Xu J, Liu Z, *et al*. Conditional inactivation of FGF receptor 2 reveals an essential role for FGF signaling in the regulation of osteoblast function and bone growth. *Development* 2003;130:3063–74.
17 Chen H, Zhuang F, Liu Y-H, *et al*. Tgf-Beta receptor II in epithelia versus mesenchyme plays distinct roles in the developing lung. *Eur Respir J* 2008;32:285–95.
18 Luo Y, Li N, Chen H, *et al*. Spatial and temporal changes in extracellular elastin and laminin distribution during lung alveolar development. *Sci Rep* 2018;8:8334.
19 Issitt T, Bosseboeuf E, De Winter N, *et al*. Neuropilin-1 controls endothelial homeostasis by regulating mitochondrial function and iron-dependent oxidative stress. *iScience* 2019;11:205–23.
20 Noller CM, Boulina M, McNamara G, *et al*. A practical approach to quantitative processing and analysis of small biological structures by fluorescent imaging. *J Biomol Tech* 2016;27:90–7.
21 Sun J, Zhuang F-F, Mullersman JE, *et al*. Bmp4 activation and secretion are negatively regulated by an intracellular gremlin-BMP4 interaction. *J Biol Chem* 2006;281:29349–56.
22 Yan M, Gingras M-C, Dunlop EA, *et al*. The tumor suppressor Folliculin regulates AMPK-dependent metabolic transformation. *J Clin Invest* 2014;124:2640–50.
23 Luo Y, El Agha E, Turcatel G, *et al*. Mesenchymal adenomatous polyposis coli plays critical and diverse roles in regulating lung development. *BMC Biol* 2015;13:42.
24 Sun L, Akiyama K, Zhang H, *et al*. Mesenchymal stem cell transplantation reverses multiorgan dysfunction in systemic lupus erythematosus mice and humans. *Stem Cells* 2009;27:1421–32.
25 Shi W, Zhao J, Anderson KD, *et al*. Gremlin negatively modulates BMP-4 induction of embryonic mouse lung branching morphogenesis. *Am J Physiol Lung Cell Mol Physiol* 2001;280:L1030–9.
26 Sundaram S, Tasker AD, Morrell NW. Familial spontaneous pneumothorax and lung cysts due to a folliculin exon 10 mutation. *Eur Respir J* 2009;33:1510–2.
27 Baba M, Hong S-B, Sharma N, *et al*. Folliculin encoded by the BHD gene interacts with a binding protein, FNIP1, and AMPK, and is involved in AMPK and mTOR signaling. *Proc Natl Acad Sci U S A* 2006;103:15552–7.
28 Schmidt LS, Linehan WM, Features C. Clinical features, genetics and potential therapeutic approaches for Birt-Hogg-Dubé syndrome. *Expert Opin Orphan Drugs* 2015;3:15–29.
29 Yan M, Audet-Walsh Étienne, Manteghi S, *et al*. Chronic AMPK activation via loss of FLCN induces functional beige adipose tissue through PGC-1α/ERRα. *Genes Dev* 2016;30:1034–46.
30 Baba M, Endoh M, Ma W, *et al*. Folliculin regulates osteoclastogenesis through metabolic regulation. *J Bone Miner Res* 2018;33:1785–98.
31 Cash TP, Gruber JJ, Hartman TR, *et al*. Loss of the Birt-Hogg-Dubé tumor suppressor results in apoptotic resistance due to aberrant TGFβ-mediated transcription. *Oncogene* 2011;30:2534–46.
32 Hoshika Y, Takahashi F, Togo S, *et al*. Haploinsufficiency of the folliculin gene leads to impaired functions of lung fibroblasts in patients with Birt-Hogg-Dubé syndrome. *Physiol Rep* 2016;4. doi:10.14814/phy2.13025. [Epub ahead of print: 15 Nov 2016].
33 Sun Z, Wang C, Shi C, *et al*. Activated Wnt signaling induces myofibroblast differentiation of mesenchymal stem cells, contributing to pulmonary fibrosis. *Int J Mol Med* 2014;33:1097–109.
34 Mathieu J, Detraux D, Kuppers D, *et al*. Folliculin regulates mTORC1/2 and Wnt pathways in early human pluripotency. *Nat Commun* 2019;10:632.
35 Kennedy JC, Khabibullin D, Henske EP. Mechanisms of pulmonary cyst pathogenesis in Birt-Hogg-Dube syndrome: the stretch hypothesis. *Semin Cell Dev Biol* 2016;52:47–52.
36 Germain DP, type E-Dsyndrome IV. Ehlers-Danlos syndrome type IV. *Orphanet J Rare Dis* 2007;2:32.
37 Urban Z, Gao J, Pope FM, *et al*. Autosomal dominant cutis laxa with severe lung disease: synthesis and matrix deposition of mutant tropoelastin. *J Invest Dermatol* 2005;124:1193–9.
38 Preston RS, Philp A, Claessens T, *et al*. Absence of the Birt-Hogg-Dubé gene product is associated with increased hypoxia-inducible factor transcriptional activity and a loss of metabolic flexibility. *Oncogene* 2011;30:1159–73.
39 Possik E, Jalali Z, Nouët Y, *et al*. Folliculin regulates AMPK-dependent autophagy and metabolic stress survival. *PLoS Genet* 2014;10:e1004273.
40 Ren S, Luo Y, Chen H, *et al*. Inactivation of TSC2 in mesoderm-derived cells causes polycystic kidney lesions and impairs lung alveolarization. *Am J Pathol* 2016;186:3261–72.
41 Medvetz DA, Khabibullin D, Hariharan V, *et al*. Folliculin, the product of the Birt-Hogg-Dube tumor suppressor gene, interacts with the adherens junction protein p0071 to regulate cell-cell adhesion. *PLoS One* 2012;7:e47842.
42 Hu Y, Fu J, Xue X. Association of the proliferation of lung fibroblasts with the ERK1/2 signaling pathway in neonatal rats with hyperoxia-induced lung fibrosis. *Exp Ther Med* 2019;17:701–8.
43 Joannes A, Brayer S, Besnard V, *et al*. Fgf9 and FGF18 in idiopathic pulmonary fibrosis promote survival and migration and inhibit myofibroblast differentiation of human lung fibroblasts in vitro. *Am J Physiol Lung Cell Mol Physiol* 2016;310:L615–29.
44 Koo HY, El-Baz LM, House S, *et al*. Fibroblast growth factor 2 decreases bleomycin-induced pulmonary fibrosis and inhibits fibroblast collagen production and myofibroblast differentiation. *J Pathol* 2018;246:54–66.